Int. J. Heat Mass Transfer. Vol. 36, No. 18, pp. 4335–4340, 1993
Printed in Great Britain

0017–9310/93 $6.00 + 0.00

Mathematical modelling of surface segregation in aluminum DC casting caused by exudation

ASBJØRN MO
SINTEF SI, Box 124 Blindern, 0314 Oslo, Norway

(*Received* 18 *November* 1992 *and in final form* 15 *June* 1993)

Abstract—A mathematical model for the development of a segregated layer of exudated droplets during DC casting of aluminum ingots is established. The model accounts for the metallostatic pressure driven interdendritic melt flow through the mushy zone by a Darcy type equation, the surface segregation due to this melt flow, and the decrease of the total solute concentration in different positions of the mush as a result of the exudation. The solution domain for the governing differential equations is constituted by the mushy zone of the cast. The main physical phenomena included in the model have been studied in a simple one dimensional case study.

1. INTRODUCTION

THE SURFACE quality of DC cast aluminum ingots is often reduced by a segregated layer of exudated droplets. Compared to the nominal content of alloying elements, the surface layer is considerably enriched, and it is believed to be a main cause of edge cracking during hot rolling of DC cast slabs [1]. Furthermore, surface segregation developed during casting of extrusion ingots can lead to large local variations in extruded profiles. The removal of the exudations before further processing of the ingot entails high costs.

This kind of surface segregation is caused by interdendritic flow of enriched liquid through the mushy zone. Two essential driving forces for surface segregation are believed to exist, namely the metallostatic pressure and forces generated by the volume expansion of the re-heated, mushy shell. Ohm and Engler [2] separated these two mechanisms experimentally, and showed that a surface segregation layer caused by volume expansion is very small compared to a layer resulting from a pressure driven exudation. Also other authors [3–6] state that surface segregation in aluminum DC casting is caused by a pressure drop through the mushy zone, and that this drop is induced by air gap formation between the partly solidified shell and the mould. A sketch of the principles of this mechanism is shown in Fig. 1.

This report is directed towards the mathematical modelling of this surface segregation phenomenon. Our aim is to establish a set of differential equations by which pressure driven interdendritic melt flow, as indicated in Fig. 1, and its interaction with the solid–liquid phase transition in the mush can be modelled.

In former studies on macrosegregation the various types such as, for example, centerline segregation and inverse segregation, were treated as separate phenomena. Flemings and Nereo [7] showed, however, that these as well as other types of macrosegregation result from the same basic mechanism, and can quantitatively be described by the same set of equations. A similar point of view lies behind the more recent literature in which the differential field equations for the mechanics of the mushy zone have been thoroughly discussed. Important references are [8–13], and several other relevant papers are cited in these references. Most of the case studies based on the mathematical field descriptions are concerned with problems in which thermal or thermo-solutal, free convection is the driving mechanism for the interdendritic melt flow. We believe, though, that the metallostatic pressure driven interdendritic melt flow in Fig. 1 could also have been modelled if pertinent boundary conditions on the pressure field were imposed. However, no such studies are known to the author.

Of particular interest to the present study is Buxmann's paper [5] in which a problem similar to ours was modelled. While Buxmann based the melt flow modelling on a global treatment of the mushy zone, we have represented the mush by a Darcy type of momentum balance differential equation with a liquid fraction dependent permeability.

Even though the basis for our modelling has been

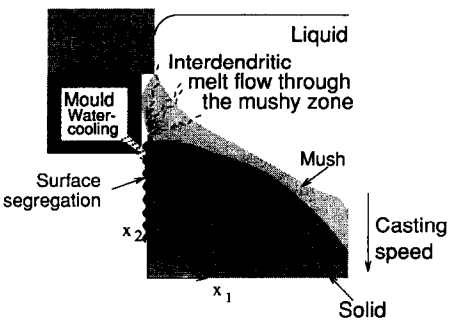

FIG. 1. Principles of the surface segregation mechanism in aluminum DC casting.

NOMENCLATURE

a	slope of the liquidus line of the phase diagram [K]
b	temperature gradient in the case study [K m^{-1}]
c	solute concentration in the liquid part of a volume element [−]
$\bar{c}$	total solute concentration in a volume element [−]
c_0	initial solute concentration [−]
$\Delta\bar{c}$	macrosegregation in the mushy zone, $\bar{c}-c_0$ [−]
c_p	specific heat [J kg^{-1} K^{-1}]
f	liquid fraction [−]
g	acceleration due to gravity [m s^{-2}]
k	equilibrium partition ratio [−]
K	permeability [m^2]
L	specific heat of fusion [J kg^{-1}]
p	pressure [N m^{-2}]
p_0	metallostatic pressure at $x = x_0$ in the case study [N m^{-2}]
r	top position of the mushy zone in the case study [m]
Δr	mean thickness of the surface layer [m]
t	time [s]
T	temperature [K]
T_{liq}	liquidus temperature [K]
T^0_{liq}	initial liquidus temperature [K]
T^{Al}_{liq}	liquidus temperature of pure aluminum [K]
V_i	superficial velocity component [m s^{-1}]
V	superficial velocity in the case study [m s^{-1}]
x_i	position vector component [m]
x	position in the case study [m]
x_0	bottom position for the mushy zone in the case study [m].

Greek symbols

δ_{ij}	Kronecker delta [−]
γ	material parameter, $\eta^2/8\pi\tau^3$ [m^2]
η	primary dendrite spacing [m]
μ	dynamic liquid viscosity [N s m^{-2}]
λ	thermal conductivity [W m^{-1} K^{-1}]
ρ	density [kg m^{-3}]
τ	tortuosity [−].

found in the differential equation literature cited above, a major intention is to simplify the mathematical description as much as possible. The model, and the assumptions behind it are discussed in Section 2, and Section 3 is devoted to a simple one dimensional case study.

2. GOVERNING EQUATIONS

Three physical phenomenon are to be accounted for by the model. These are the forced convection of the interdendritic melt flow due to the pressure drop through the mushy zone, the surface segregation caused by this melt flow, and the decrease of the total solute concentration, i.e. the macrosegregation, as a result of the exudation. It should be noted that the decrease of the total solute concentration leads to a decrease in liquid fraction, i.e. solidification.

We apply a frame of reference moving with the same velocity as the completely solidified part of the cast. The spatial coordinates are denoted by x_i ($i = 1, 2, 3$) (cf. Fig. 1) and t is time. The volume averaged, or superficial, velocity, V_i is applied as the measure for melt motion. Since forces generated by volume expansion are of minor importance, we assume that the solid and liquid densities are constant and equal. This means that the continuity equation reduces to

$$\frac{\partial V_i}{\partial x_i} = 0. \tag{1}$$

The solid part of the mush is assumed to be interconnected and moving with the same speed as the completely solidified part of the cast, and no deformation of this solid matrix takes place. The momentum balance in the mush is modelled by a Darcy type equation

$$\frac{\mu V_i}{K} + \frac{\partial p}{\partial x_i} + \rho g \delta_{i2} = 0 \tag{2}$$

where the permeability K is dependent on the liquid fraction. p, ρ, g and μ are here the pressure, the density, the acceleration due to gravity and the dynamic liquid viscosity respectively, and δ_{ij} is the Kronecker delta.

The solution domain for the melt flow problem is restricted to the mush by imposing the pressure along the liquidus isotherm as a boundary condition, and assuming this pressure to be equal to the known metallostatic pressure. This assumption implies that the interaction between the studied forced convective flow and any free convection in the interdendritic melt or in the liquid above the mush resulting from buoyancy forces is neglected.

Close to the liquidus isotherm, it might be somewhat inaccurate to neglect this interaction since the pressure drop associated with the forced convection decreases with increasing permeability. In industrial aluminum alloys, typical values of the density difference between 'hot' and 'cold' or between 'pure' and 'enriched' regions are of the order 100 kg m^{-3}. The buoyancy force, which is represented by a gravity multiplied by this density difference term, is therefore of the order 10^3 N m^{-3}. However, the pressure gradi-

ent will increase and become considerably larger than the buoyancy forces as the permeability decreases. A metallostatic head of for example 0.04 m acting on a mush of thickness 0.1 m leads to a total pressure gradient through the mush of the order of 10^4 N m^{-3} which is 10 times larger than the buoyancy forces.

It should be noted that the position of the mush–liquid boundary is determined by the time evolution of the temperature field. The position will furthermore be changed by a change in the total solute concentration at the mush boundary, even if the temperature is constant.

The other boundaries are the mush–solid, mush–air and mush–mould/hot top interfaces (cf. Fig. 1). p equals zero along the mush–air interface, and along the mush–solid and mush–mould/hot top interfaces, the normal component of the superficial velocity equals zero.

Different relations between the permeability, K, and the liquid fraction, f, exist in the literature (see for example [14–19]). In the case study in Section 3 we have simply assumed the permeability to be proportional to the liquid fraction squared as derived and applied by Mehrabian *et al.* [20] in the modelling of interdendritic fluid flow under influence of gravity.

We restrict the study to a binary alloy, and model the solidificaton by the Scheil equation written in the form

$$\frac{\partial \bar{c}}{\partial t} = f\frac{\partial c}{\partial t} + (1-k)c\frac{\partial f}{\partial t} \tag{3}$$

where $\bar{c}$ is the total solute concentration, c the solute concentration in the liquid part of the mush and $k = k(c)$ the equilibrium partition ratio. We furthermore assume that solute enters or leaves the volume element by liquid flow only. This combined with the continuity equation (1) and equation (3) yields the so-called local solute redistribution equation

$$f\frac{\partial c}{\partial t} + V_l\frac{\partial c}{\partial x_i} + (1-k)c\frac{\partial f}{\partial t} = 0. \tag{4}$$

It should be noted that the Scheil description requirement of thermodynamic equilibrium at the solid–liquid interfaces is violated in a remelting situation if the mean liquid concentration has become different from what it was during the solidification [21]. As a result of this, one has to quantify the solute concentration locally in the grains or the dendritic structure during solidification if Scheil's equation is to be invoked in a macrosegregation modelling [9, 21–23].

The field quantities f and V_l appear in the energy balance equation for our problem and represents there the mathematical coupling between the evolution of the temperature field and the above discussed interdendritic flow and segregation problems. This coupling disappears, however, if heat transfer due to the forced advection of the melt is neglected, and f in the energy equation is approximated by a function uniquely given by the temperature (cf. for example [24]). In the rest of this report the temperature field and thereby the liquid concentration field are therefore regarded as known and input to the governing equations (1), (2) and (4).

3. A ONE DIMENSIONAL CASE STUDY

All main phenomena (i.e. the pressure driven interdendritic melt flow, the macrosegregation in the mush, and the surface segregation) of the above outlined mathematical model can be studied in the simple one dimensional case study sketched in Fig. 2. The spatial coordinate is denoted by x, and the boundary having temperature equal to the liquidus temperature is initially situated at $x = 0$. The thickness of the mushy zone is then 0.03 m, and the exudation is modelled for a period of 100 s. The pressure at $x = 0$ is 2340 N m^{-2} (which corresponds to a metallostatic head of 0.1 m) throughout the process. It should be noted that this model problem is very similar to the surface exudation problem studies experimentally by Ohm and Engler [2].† The mushy zone thickness and the metallostatic head are therefore chosen in accordance with values applied in this reference.

For simplicity we have assumed the temperature to be stationary and related to x by

$$T = T^0_{liq} - bx \tag{5}$$

where $b = 2600$ K m^{-1} and T^0_{liq} equals the initial value of the liquidus temperature, 905.5 K (632.5°C). The decrease in solute content in the mush due to the exudation leads to a solidification in spite of the stationary temperature conditions. The increased value of the liquidus temperature resulting from the decrease in solute content results furthermore in a drift in negative x direction of the boundary initially situated at $x = 0$.

The alloy in the case study is Al–5% Mg. We find from the Al–Mg phase diagram [25, p. 24] that the relation between the liquid concentration and the temperature, T, can be approximated by

$$c = \frac{1}{a}(T^{Al}_{liq} - T) \tag{6}$$

where $T^{Al}_{liq} = 933$ K (660°C) is the liquidus temperature of pure aluminum, and a is approximated by the constant 550 K. c as a function of x (cf. Fig. 2) which is input to the differential equations of the model, can then easily be calculated from equations (5) and (6). The partition coefficient, k, is approximated by the constant 0.41.

† Due to lack of quantitative measurements, it is unfortunately not possible to use the results in ref. [2] for experimental validation of the modelling.

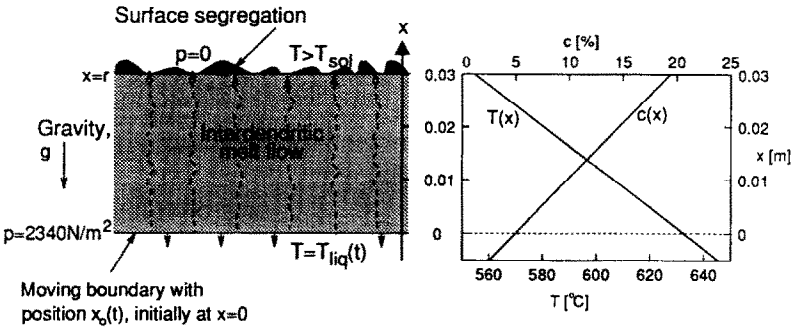

FIG. 2. Principals of the one dimensional model problem.

3.1. *Solution of the equations*

Since the temperature field, and thereby the liquid concentration field, is stationary, the governing differential equations (1), (2) and (4) reduce to

$$\frac{\partial V}{\partial x} = 0 \tag{7}$$

$$\frac{\mu V}{K} + \frac{\partial p}{\partial x} + g\rho = 0 \tag{8}$$

$$V\frac{\partial c}{\partial x} + (1-k)c\frac{\partial f}{\partial t} = 0 \tag{9}$$

where V is the superficial velocity. The pure solidification situation (no remelting) secures that the solidification can be handled by the proposed Scheil description without any need to trace the local solid solute concentration during solidification. In accordance with the Scheil description of the solidification, the initial condition for f in the mush as a function of c is

$$f(x,0) = \left[\frac{c(x)}{c_0}\right]^{(1/(k-1))} \qquad 0 \leqslant x \leqslant r \tag{10}$$

where r is the top position of the mushy zone and $c_0 = 0.05$. $f(x, 0)$ equals 1 (pure liquid) when $x < 0$. In the modelling results presented below ρ and μ are 2385 kg m^{-3} and 1.2×10^{-3} N s m^{-2} respectively [26, p. 944].

From equation (7) it is seen that $V(t)$ is independent of x. By integrating equation (9) with respect to t and equation (8) with respect to x from the current bottom position, $x_0(t)$ to the top position, r of the mushy zone, we obtain

$$f(x,t) = f(x,0) - \frac{1}{1-k}\int_0^t V(t)\frac{1}{c}\frac{\partial c}{\partial x}\partial t \tag{11}$$

and

$$V(t) = \frac{p_0(t) + \rho g x_0(t) - \rho g r}{\mu \int_{x_0(t)}^{r} \frac{\partial x}{K[f(x,t)]}}. \tag{12}$$

$p_0(t)$ is here the metallostatic pressure at $x_0(t)$, and we note that $p_0(t) + \rho g x_0(t)$ equals the known pressure (2340 N m^{-2}) at $x = 0$.

$f(x, t)$ has been determined by a numerical calculation of the integral (11) with $V(t)$ updated between every time step by equation (12). A mid point integration scheme has been applied in the spatial integration. $x_0(t)$ is given by inserting the current value of the liquidus temperature, $T_{liq}(t)$, into equation (5). $T_{liq}(t)$ is updated between every time step by replacing c in equation (6) with the current value of the total solute concentration, $\bar{c}$ (cf. equation (3) with $\partial c/\partial t = 0$), at the current mush boundary.

3.2. *Calculation of segregation*

The mean thickness of the surface layer which develops at $x = r$ constitutes a measure of the surface segregation. The mean thickness, Δr, is given by

$$\Delta r = \int_0^t V(t)\partial t. \tag{13}$$

The total solute concentration in this layer is equal to $c(r) \approx 0.19$ (cf. Fig. 2).

The macrosegregation in the mushy zone, $\Delta\bar{c}$, as a function of time is given by the difference between the total solute concentration at time t and at $t = 0$. Integration of equation (3) in which the time derivative of c is zero, with equation (9) inserted yields

$$\Delta\bar{c} = -\int_0^t \frac{\partial c}{\partial x} V(t)\partial t. \tag{14}$$

We note that the special case of constant gradient $\partial c/\partial x$ leads to a $\Delta\bar{c}$ which is independent of x.

3.3. *Modelling results*

There is a lack of quantitative permeability data for mushy aluminum alloys. In their study of the interdendritic melt flow in a Pb–20% Sn alloy, Streat and Weinberg [15] derived the relation

$$K = \frac{\eta^2 f^2}{8\pi\tau^3} = \gamma f^2 \tag{15}$$

where η is the primary dendrite spacing and τ the tortuosity. They determined τ to be 4.6 for values of

η ranging from 20 to 100 μm. $\eta = 60$ μm then leads to $\gamma \approx 1.5 \times 10^{-12}$ m^2.

It is of course questionable whether this γ-value measured for Pb–20%Sn is applicable to the modelling of Al–5%Mg, particularly because τ frequency is considered to lie between 1.4 and 2 which is considerably lower than Streat and Weinberg's measured value. Since $\tau = 1.4$ gives $\gamma \approx 60 \times 10^{-12}$ m^2 (when $\eta = 60$ μm), it becomes clear that a quite different value of γ might be the correct one in the present case study.

Instead of making any further speculations on what the value of γ should be, we have *chosen* its value to be 1×10^{-12}, 10×10^{-12} and 100×10^{-12} m^2 respectively. We have then studied the modeling results for the mean thickness of the surface layer defined by equation (13) and the macrosegregation in the mush defined by equation (14) for these three γ-values.

From equation (12) it is seen that the largest γ-value gives the largest value of V and thereby the most significant surface segregation and macrosegregation. The high segregation leads rapidly to a pronounced decrease in the liquid fraction and a corresponding decrease of the melt flow. This effect is reflected in Fig. 3 where we see that Δr and the absolute value of $\Delta \bar{c}$ for $\gamma = 100 \times 10^{-12}$ m^2 have a rapid increase during the first 30 s followed by a much slower increase. For the lower values of γ there is on the other hand a more steady but slower growth of both Δr and $|\Delta \bar{c}|$.

In the proceeding part of the discussion we have taken γ to be its intermediate value equal to 10×10^{-12} m^2. We see from Fig. 3 that this leads to a mean thickness of the surface segregation layer after 100 s

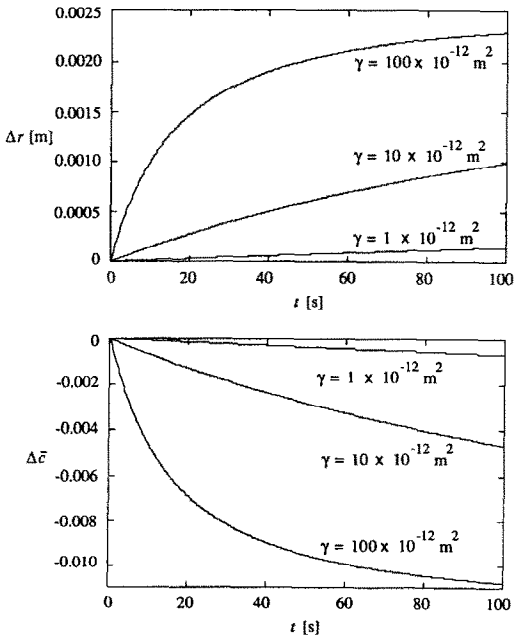

FIG. 3. Mean thickness of the exudated surface segregation layer and macrosegregation in the mushy zone as functions of time for different values of γ.

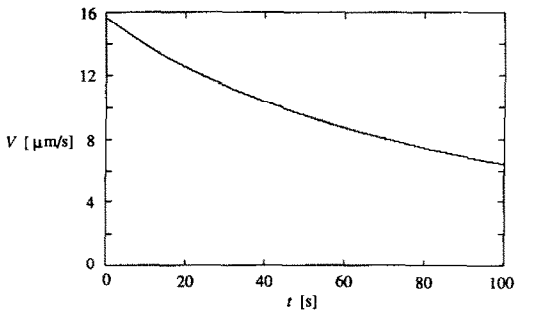

FIG. 4. Velocity of the melt into the mush as a function of time ($\gamma = 10 \times 10^{-12}$ m^2).

approximately equal to 1 mm. It is furthermore seen that $\Delta \bar{c} \approx -0.005$ after 100 s when $\gamma = 10 \times 10^{-12}$ m^2. The total solute concentration has in other words decreased from the initial 5% down to approximately 4.5%.

$V(t)$ is shown in Fig. 4, and it is seen how $V(t)$ decreases as time proceeds. This result corresponds to the decrease in liquid fraction being revealed in Fig. 5. Also the drift in the position of the 'hot' boundary of the mushy zone is seen in Fig. 5. While $x = 0$ is the initial position for $f = 1$, it turns out that f equals one at approximately -0.001 m after 100 s.

When the velocity V has been determined, it is of interest to compare the advective transport of thermal energy with the diffusive energy flux. While the latter of these is given by Fourier's law, $\lambda(\partial T/\partial x)$, where the conductivity, λ, is approximated by 100 W m^{-1} °C^{-1}, the advective heat flux is $\rho c_p TV$ where the heat capacity, c_p, is 1080 J kg^{-1} °C [26, p. 941]. With $\partial T/\partial x = b = 2600$°C m^{-1}, $T \sim 1000$ K and $V \sim 10^{-5}$ m s^{-1} this means that the diffusive energy transport is approximately 10 times larger than the advective transport. This result is in agreement with the assumption made in Section 2 of neglecting the temperature change, and thereby the change of c, due to thermal advection. It should, however, be emphasized that the above consideration does not generally justify the assumption of neglecting the advection of thermal energy. While a decrease in temperature gradient leads

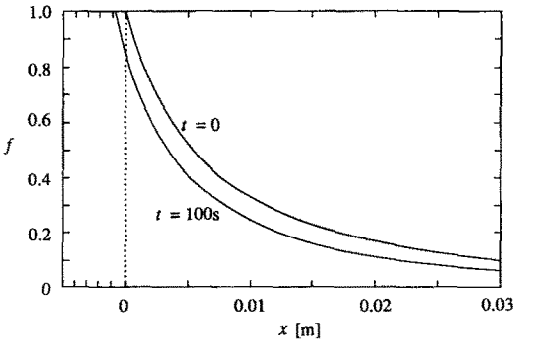

FIG. 5. Liquid fraction in the mushy zone at $t = 0$ s and $t = 100$ s ($\gamma = 10 \times 10^{-12}$ m^2).

to decreased diffusion, there is no reason for a temperature gradient decrease to lead to a decrease in V.

4. CONCLUSION

- A mathematical model for the development of a segregated layer of exudated droplets during DC casting of aluminum ingots is established.
- Assuming the temperature field and its evolution with time as known, it has been pointed out how the model can quantify the interdendritic melt flow through the mushy zone and the interaction between this flow and the solid–liquid phase transition in the mush. Hence, also the decrease of the total solute concentration in different positions of the mush as a result of the exudation can be determined.
- The main physical phenomena included in the model have been studied in a simple one dimensional case study.

Acknowledgement—This research has been funded by Elkem Aluminum and The Royal Norwegian Council for Scientific and Industrial Research. The author is very grateful for the stimulating collaboration with Einar Jensen at Elken Research. He has also had numerous discussions with Tor Johnsen, Yngve Langsrud and Bjørn Andersson all at SINTEF SI pertaining the metallurgical basis for the research, and thank each of them for sharing their insight. Per Kolby at SINTEF SI is acknowledged for proof reading the manuscript.

REFERENCES

1. I. H. Hove, B. Andersson and D. Voss, Edge cracking during hot rolling of A15Mg. In *Proceedings from the 3rd Conference on Aluminium Alloys—Their Physical and Mechanical Properties* (Edited by L. Arnberg, O. Lohne, E. Nes and N. Ryum), Vol. 2, pp. 264–269, Trondheim, June (1992).
2. L. Ohm and S. Engler, Treibende Kräfte der Oberflächensiegrungen beim NE-Stranguß, *Metall.* **43**(6), 520–524 (1989).
3. H. Kästner, Die umgekehrte Blockseigrung bei Strangguß I, *Zeitschrift für Metallkunde* **41**(7), 193–205 (1950).
4. H. Kästner, Die umgekehrte Blockseigrung bei Strangguß II, *Zeitschrift für Metallkunde* **41**(8), 247–254 (1950).
5. K. Buxmann, Mechanismen der Oberflächenseigrung von Strangguß, *Metall.* **31**(2), 163–170 (1977).
6. R. Ellerbrok and S. Engler, Untersucherungen zur Oberflächenseigrung von Stranggußlegierungen *Metall.* **37**(8), 784–788 (1983).
7. M. C. Flemings and G. E. Nereo, Macrosegregation, Part I, *Trans. Metall. Soc. AIME* **239**, 1449–1461 (1967).
8. W. D. Bennon and F. P. Incropera, A continuum model for momentum, heat and species transport in binary solid liquid phase change systems—I. Model formulation, *Int. J. Heat Mass Transfer* **30**, 2161–2170 (1987).
9. V. R. Voller, A. D. Brent and C. Prakash, The modelling of heat, mass and solute transport in solidification systems, *Int. J. Heat Mass Transfer* **32**, 1719–1732 (1989).
10. S. Ganesan and D. R. Poirier, Conservation of mass and momentum for the flow of interdendritic liquid during solidification, *Metall. Trans.* **21B**, 173–181 (1990).
11. R. Viskanta, Mathematical modeling of transport processes during solidification of binary systems (Review), *JSME Int. J.* **33**(3), 409–423 (1990).
12. P. J. Prescott, F. P. Incropera and W. D. Bennon, Modelling of dendritic solidification systems: reassessment of the continuum momentum equation, *Int. J. Heat Mass Transfer* **34**(9), 2351–2359 (1991).
13. J. Ni and C. Beckermann, A volume-averaged two-phase model for transport phenomena during solidification, *Metall. Trans.* **22B**, 349–361 (1991).
14. D. Apelian, M. C. Flemings and R. Mehrabian, Specific permeability of partially solidified dendritic networks of Al Si alloys, *Metall. Trans.* **5**, 2533–2537 (1974).
15. N. Streat and F. Weinberg, Interdendritic fluid flow in a lead–tin alloy, *Metall. Trans.* **7B**, 417–423 (1976).
16. K. Murakami and T. Okamoto, Fluid flow in the mushy zone composed of granular grains, *Acta Metall.* **32**(10), 1741–1744 (1984).
17. R. West, On the permeability of the two-phase zone during solidification of alloys, *Metall. Trans.* **16A**, 693 (1985).
18. D. R. Poirier, Permeability for flow of interdendritic liquid in columnar-dendritic alloys, *Metall. Trans.* **18B**, 245–255 (1985).
19. D. R. Poirier and S. Ganesan, Permeabilities for flow of interdendritic liquid in equiaxial structures, *Materials Sci. Engng* **A157**, 113–123 (1992).
20. R. Mehrabian, M. Keane and M. C. Flemings, Interdendritic fluid flow and macrosegregation. Influence of gravity, *Metall. Trans.* **1**, 1209–1220 (1970).
21. M. Rappaz and V. Voller, Modelling of micro-macrosegregation in solidification processes, *Metall. Trans.* **21A**, 749–753 (1990).
22. Daming Xu and Quigchun Li, Numerical method for solution of strongly coupled binary alloy solidification problems, *Numer. Heat Transfer* **20A**, 181–201 (1991).
23. Quiping Yu and Yaohe Zhou, Numerical simulation of convection in the two-phase zone of a binary alloy, *Int. J. Heat Mass Transfer* **34**(3), 843–852 (1991).
24. M. Rappaz, Modelling of microstructure formation in solidification processes, *Int. Materials Rev.* **34**(3), 93–123 (1989).
25. *Equilibrium Diagrams of Aluminium Alloy Systems*, Information Bulletin No. 25, The Aluminum Development Association, December (1961).
26. C. J. Smithells, *Metals Reference Book* (5th Edn). Butterworths, London and Boston (1976).